

Two-dimensional rigid polycrystals whose grains have one ductile direction

BY GUILLERMO H. GOLDSZTEIN

*Georgia Institute of Technology, School of Mathematics,
686 Cherry Street, Atlanta, GA 30332-0160, USA*

*Received 18 December 2001; revised 31 October 2002; accepted 19 November 2002;
published online 11 June 2003*

We consider polycrystals with perfectly plastic grains. We study the two-dimensional problem that results if the textures and applied stresses are compatible with anti-plane deformation. We show that the order of magnitude of recently introduced outer bounds on the strength domain of polycrystals is sharp even under the assumption of square symmetry on the texture. We also conclude that the fact that the texture has square symmetry is not enough information to predict the behaviour of polycrystals if the grains are highly anisotropic.

Keywords: plasticity; polycrystals; strength domain; macroscopic behaviour

1. Introduction

Single crystals are materials whose atoms form a periodic lattice. A consequence of the periodicity of the atomic lattice is that single crystals are generally anisotropic. Metals are usually found in the form of polycrystals, that is, large collections of bonded grains where each grain is a single crystal. Since the orientation of the atomic lattice varies from grain to grain, the material properties of polycrystals depend not only on the properties of the grains, but also on the polycrystalline texture, i.e. shape, orientation and spatial distribution of the grains.

Growing large single crystals is expensive and difficult; consequently, in most applications, crystalline materials are used in polycrystalline form. The properties of polycrystals may differ substantially from those of the corresponding single crystal. Any isotropic polycrystal whose grains are highly anisotropic is a good example. Furthermore, polycrystals of the same material but with different textures may also exhibit different properties. Since the texture can be partly controlled, it is valuable to predict the dependence of the properties of polycrystals on their texture to provide guidelines in material selection and processing.

The stresses that an homogeneous elastic–perfectly plastic material can withstand form a closed set K in the space of symmetric 3×3 real matrices. K is called the yield set or strength domain. The material experiences elastic deformations when subjected to a stress σ that is in the interior of K (the material returns to its original form when the applied stress σ is removed). On the other hand, if $\sigma \in \partial K$ (the boundary of K), the material experiences plastic deformation and continues deforming until the stress is removed (this is a permanent deformation). If the material is a single crystal, the set K is convex and is related to the slip systems, which in turn depend

on the atomic lattice (Hirth & Lothe 1982; Lubliner 1990). The grains of a large class of metals can be considered to be elastic–perfectly plastic (Hirth & Lothe 1982; Lubliner 1990; Bolton 1996).

The texture of a polycrystal is determined by a rotation-valued function $R(x)$. More precisely, $R(x)$ denotes the orientation of the grain (i.e. the orientation of the atomic lattice within the grain) that contains the point x .

If the yield set of the reference single crystal is K , then RKR^T is the yield set of a single crystal whose orientation is R . Thus, a polycrystal can only withstand stresses σ that satisfy the point-wise constraint

$$R^T(x)\sigma(x)R(x) \in K \quad (1.1)$$

in addition to the equilibrium equations

$$\nabla \cdot \sigma = 0. \quad (1.2)$$

Suppose that $R(x)$ is periodic with period cell Q and that Ω is the region occupied by the polycrystal. A stress field σ is said to be admissible if it is Q -periodic and satisfies (1.1) and (1.2). In the limit in which the dimensions of Q are much smaller than those of Ω , a polycrystal, whose grains are elastic–perfectly plastic, behaves as a material that can only withstand *macroscopic* stresses in K_{hom} , where

$$K_{\text{hom}} = \{\tau : \tau = \langle \sigma \rangle, \text{ for some admissible } \sigma\}. \quad (1.3)$$

In the above equation we have used the notation

$$\langle f \rangle = |Q|^{-1} \int_Q f(x) dx.$$

See Suquet (1982, 1983, 1987, 1988), de Buhan (1986), Bouchitté & Suquet (1991), de Buhan & Taliercio (1991), Demengel & Qi (1990), Jikov *et al.* (1994) and Sab (1994) for a more detailed discussion.

The set K_{hom} is called the strength domain of the polycrystal. Note that K_{hom} does not depend on the elastic moduli of the grains, but only on the yield set of the reference single crystal K and the texture $R(x)$. If the polycrystal is subjected to a stress in the interior of K_{hom} , some plastic deformation may (and, in general, does) occur. However, this plastic deformation is localized and limited, i.e. the polycrystal reaches a certain shape and does not deform further if the stress remains constant. Once the stress is removed, the polycrystal is left with some permanent deformation and residual stresses that do depend on the elastic moduli of the grains. If the polycrystal is subjected to stress in ∂K_{hom} , it deforms and continues to do so until the stress is removed.

A two-dimensional problem results from considering polycrystals with texture and under applied stresses compatible with anti-plane deformation. More precisely, assume that each grain has the shape of an infinite cylinder whose axis is parallel to the x_3 -axis, that $R(x)$ is independent of x_3 and keeps the x_3 -axis fixed, and that we restrict our attention to average stresses whose component $\langle \sigma_{ij} \rangle$ may only be non-zero if $i \neq j$ and one of the indexes (i or j) is equal to 3. Thus, due to symmetry, we can assume that $\sigma_{ij}(x)$ may only be non-zero if $i \neq j$ and one of the indexes is equal to 3. Under these conditions, (1.1)–(1.3) become a two-dimensional problem. More precisely, rename the non-zero components of the stress as $\sigma_i = \sigma_{i3}$ ($i = 1, 2$)

and denote by σ the two-dimensional vector whose components are σ_1 and σ_2 . The yield set of the reference single crystal is now a convex set in \mathbb{R}^2 , that we also denote by K , and the condition (1.1) reduces to

$$R^T(x)\sigma(x) \in K, \quad (1.4)$$

where $R(x)$ is now a 2×2 rotation and $x \in \mathbb{R}^2$ is in the intersection of the polycrystal with the plane $x_3 = 0$. Thus, we now say that σ is admissible if it is Q -periodic (Q is the period cell of $R(x)$) and satisfies (1.2) and (1.4). The strength domain of the polycrystal K_{hom} is still given by (1.3) but now K_{hom} is a subset of \mathbb{R}^2 .

Note that the rotation $R(x)$ is determined by an angle $\theta(x)$,

$$R(x) = R_{\theta(x)} = \begin{bmatrix} \cos(\theta(x)) & -\sin(\theta(x)) \\ \sin(\theta(x)) & \cos(\theta(x)) \end{bmatrix}. \quad (1.5)$$

We will sometimes refer to θ as the texture of the polycrystal.

Kohn & Little (1998) studied the above-described two-dimensional polycrystal in the case in which the yield set of the reference single crystal is

$$K = \{\sigma \in \mathbb{R}^2 : |\sigma_1| \leq M \text{ and } |\sigma_2| \leq 1\}. \quad (1.6)$$

The parameter M in equation (1.6) is a measure of the anisotropy. As M becomes large, the single crystal with yield set (1.6) becomes rigid in one direction (i.e. it can withstand stresses of the form $(\sigma_1, 0)$, where σ_1 may be large, $|\sigma_1| \leq M$) but remains ductile in the orthogonal direction (i.e. if the stress is of the form $(0, \sigma_2)$, we have $|\sigma_2| \leq 1$).

A number of schemes have been developed to estimate the mechanical properties of nonlinear composite materials and polycrystals with nonlinear grains (Sachs 1928; Taylor 1938; Bishop & Hill 1951; Hutchinson 1976; Willis 1983; Talbot & Willis 1985; Ponte Castañeda 1991, 1996; Dendievel *et al.* 1991; Suquet 1993; Lebensohn 1993, 1999; Olson 1994; deBotton & Ponte Castañeda 1995). A review of some of these methods is given in Ponte Castañeda & Suquet (1997). However, no single estimate can be effectively applied to every material. Moreover, the accuracy of these approximations is sometimes uncertain.

The two-dimensional model (1.2)–(1.6) is amenable to mathematical analysis and retains the important effects of nonlinearity and those associated with texture. Thus, it is an ideal model to test the schemes mentioned above, develop new ones and gain intuition on the behaviour of real materials. These facts are reflected in the large number of researchers that have studied this model soon after Kohn & Little (1998) introduced it (Ponte Castañeda & Nebozhyn 1997; Nesi *et al.* 2000; Goldsztein 2001).

Kohn & Little (1998) proved that, if K_{hom} is invariant under rotation by $\pi/2$, then $K_{\text{hom}} \subseteq B_{\sqrt{2M}}$, where $B_r \subseteq \mathbb{R}^2$ denotes the ball of radius r centred at the origin. The estimate computed by Ponte Castañeda & Nebozhyn (1997), which is valid for isotropic polycrystals, approximates K_{hom} by a ball of radius $O(\sqrt{M})$ smaller than the Kohn & Little (1998) bound. Nesi *et al.* (2000) improved upon the Kohn & Little (1998) bound under the assumption that the polycrystal is isotropic. However, their bound seems to coincide with the Kohn & Little (1998) bound for values of M larger than 3.5.

In real applications it is desirable to produce polycrystals that can withstand large stresses in all directions. A polycrystal can withstand stresses of norm ρ in all

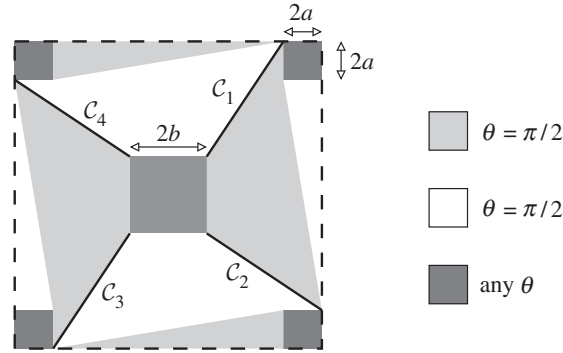


Figure 1. Texture of the polycrystals to be considered.

directions if and only if $\rho \leq \rho^*$, where

$$\rho^* = \max_{B_\rho \subseteq K_{\text{hom}}} \rho. \tag{1.7}$$

Note that $K_{\text{hom}} = B_{\rho^*}$ if the polycrystal is isotropic.

Goldsztein (2001) showed that $\rho^* \leq 4\sqrt{M}/\pi$. On the other hand, for each value of M , Goldsztein constructed a polycrystal whose strength domain contains the set $[-f, f] \times [-f, f]$, where $f = \sqrt{M} - O(1)$. This shows that a bound of the form $\rho^* \leq \rho_u$ that is valid for all polycrystals necessarily satisfies $\rho_u \geq \sqrt{M} - O(1)$ and thus, the order of magnitude of the bound obtained by Kohn & Little (1998) is sharp for large values of M .

However, it is not known if the above-mentioned bounds can be improved if symmetry assumptions are made on the texture. Moreover, as pointed out by Kohn & Little (1998), it is not known if there exists a polycrystal that becomes rigid in all directions as $M \rightarrow \infty$. In other words, fix the texture $\theta = \theta(x)$ and regard M as a variable. Thus, $\rho^* = \rho^*(M)$ becomes a function of M . It is not known if there exists a texture θ for which $\lim_{M \rightarrow \infty} \rho^*(M) = \infty$.

In this paper we resolve the above issues. More precisely, we show that, for any $0 < \lambda < 1/2$, there exists a polycrystal whose texture θ has square symmetry and satisfies $\lim_{M \rightarrow \infty} \rho^*(M)/M^\lambda = C$, where $0 < C < \infty$. In particular, our results imply that the order of magnitude of the bound of Kohn & Little (1998) is sharp even under the assumption that the texture has square symmetry. We also conclude that the fact that the texture has square symmetry is not enough information to predict the behaviour of polycrystals. Some polycrystals remain ductile for all values of M (Kohn & Little 1998) and other polycrystals, such as the ones introduced in this work, become rigid as $M \rightarrow \infty$.

In §2 we introduce the polycrystals under consideration, state the results we obtained and describe the content of the rest of this paper.

2. Texture and results

Figure 1 shows the texture θ of the polycrystals we will consider. The square enclosed by dashed lines is the period cell $Q = [-1, 1]^2$. This texture is invariant under rotation by $\pi/2$, i.e. $\theta(x^\perp) + \pi/2 = \theta(x) + k\pi$, where we have used the notation $(x_1, x_2)^\perp = (x_2, -x_1)$ and k is an integer (θ is defined modulus π because the yield

set of the reference single crystal (1.6) is invariant under rotation by π). The value of θ within the white regions is zero and within the light shaded regions is $\pi/2$. The value of θ within the dark shaded regions (five squares) is irrelevant for our purposes. The boundaries between regions of different shades are straight segments except for the solid lines, i.e. the curves $\mathcal{C}_1, \mathcal{C}_2, \mathcal{C}_3$ and \mathcal{C}_4 are not necessarily straight segments. We parametrize these curves as

$$\left. \begin{aligned} \mathcal{C}_1 : z_1(t) &= (g(t), t), \\ \mathcal{C}_2 : z_2(t) &= (t, -g(t)), \\ \mathcal{C}_3 : z_3(t) &= (-g(t), -t), \\ \mathcal{C}_4 : z_4(t) &= (-t, g(t)), \end{aligned} \right\} \quad (2.1)$$

where $t \in [b, 1]$.

Let $(t_i)_{0 \leq i}$ be the sequence defined by $t_0 = 1$ and $t_{i+1} = g(t_i)$ for all $i \geq 0$. We will require the function g to satisfy the following: g is continuous and is defined in $[b, 1]$; $t_1 = 1 - 2a$; $t_{i+1} < t_i$ for all i ; g is linear within (t_{i+1}, t_i) for all i ; $g(b) = b$ and $0 < g'(t) < 1$ for all t where g' is defined. We will also require $3a < 1$ and $1 - 2a > b$.

In § 3 we will derive a relationship between an outer bound on the strength domain of polycrystals that belong to the class described above and the function g . In § 4 we will obtain an analogous result that relates an inner bound with g . These formulae will be evaluated for different choices of g in § 5. In particular, we will show that, if g is linear,

$$\{\|\tau\|_1 \leq C_0 \log M - D_0\} \subseteq K_{\text{hom}} \subseteq \{\|\tau\|_\infty \leq C_0 \log M + E_0\}, \quad (2.2)$$

where $\|\tau\|_1 = |\tau_1| + |\tau_2|$, $\|\tau\|_\infty = \max\{|\tau_1|, |\tau_2|\}$ and C_0, D_0 and E_0 are constants that depend on a and b but are independent of M . C_0 is explicitly obtained in § 5. We also show that for each $0 < \alpha$ there exists a particular choice of g , so that

$$\{\|\tau\|_1 \leq C_\alpha M^{1/(2+\alpha)} - D_\alpha A_M\} \subseteq K_{\text{hom}} \subseteq \{\|\tau\|_\infty \leq C_\alpha (2M)^{1/(2+\alpha)} + E_\alpha A_M\}, \quad (2.3)$$

where C_α, D_α and E_α are constants independent of M , and

$$A_M = \begin{cases} 1 & \text{if } \alpha > 1, \\ \log(M) & \text{if } \alpha = 1, \\ M^{(1-\alpha)/(2+\alpha)} & \text{if } \alpha < 1. \end{cases} \quad (2.4)$$

C_α is explicitly obtained in § 5. Note that equation (2.3) implies the result described in the introduction, i.e. for any $0 < \lambda < 1/2$, there exists a polycrystal whose texture θ has square symmetry and satisfies $\lim_{M \rightarrow \infty} \rho^*(M)/M^\lambda = C$, where $0 < C < \infty$ and ρ^* was defined in equation (1.7).

3. Outer bound

(a) Relationship between cuts and outer bounds

Let θ be a $[-1, 1]^2$ -periodic texture (not necessarily the one described in § 2). For convenience, we define $e(\theta) = (\cos(\theta), \sin(\theta))$ and since θ is a function of the position

x , we will also use the notation $e(x) = e(\theta(x))$. Note that the restriction (1.4) can be written as

$$|e(x) \cdot \sigma(x)| \leq M \quad \text{and} \quad |e(x)^\perp \cdot \sigma(x)| \leq 1. \quad (3.1)$$

To compute outer bounds on the strength domain of polycrystals, we will make use of the following proposition.

Proposition 3.1. *Let $z = (z_1, z_2) \in \mathbb{R}^2$ be a vector whose components are even integers. Let $\gamma : [0, 1] \rightarrow \mathbb{R}^2$ be a continuous function that satisfies $\gamma(1) - \gamma(0) = -z^\perp = (-z_2, z_1)$, the number of points where γ is not differentiable is finite, and the intersection of $\gamma([0, 1])$ with the points of discontinuities of θ is also a finite set. Then, for any admissible stress field σ (i.e. σ is $[-1, 1]^2$ -periodic and satisfies (1.2) and (3.1)), we have*

$$\langle \sigma \rangle \cdot z \leq \int_0^1 |e(\gamma(s)) \cdot \dot{\gamma}(s)^\perp| M + |e(\gamma(s)) \cdot \dot{\gamma}(s)| \, ds. \quad (3.2)$$

In the above equation $\dot{\gamma}(s)$ denotes the derivative of $\gamma(s)$. The proof of this proposition can be found in Kohn & Little (1998); however, we include a proof here for completeness.

Proof. If σ is divergence free and $[-1, 1]^2$ -periodic, $\sigma = \langle \sigma \rangle + (\nabla \psi)^\perp$ for some $[-1, 1]^2$ -periodic function ψ . Thus,

$$\int_0^1 \sigma(\gamma(s)) \cdot \dot{\gamma}(s)^\perp \, ds = - \int_0^1 \langle \sigma \rangle^\perp \cdot \dot{\gamma}(s) \, ds + \int_0^1 \nabla \psi(\gamma(s)) \cdot \dot{\gamma}(s) \, ds. \quad (3.3)$$

Since the first integral in the right-hand side of equation (3.3) is equal to $\langle \sigma \rangle \cdot z$ and the second integral is equal to 0 we have

$$\int_0^1 \sigma(\gamma(s)) \cdot \dot{\gamma}(s)^\perp \, ds = \langle \sigma \rangle \cdot z. \quad (3.4)$$

It follows from the restriction (3.1) that $|\sigma(x) \cdot v| \leq |e(x) \cdot v| M + |e(x)^\perp \cdot v|$ for any admissible stress field σ and any $x, v \in \mathbb{R}^2$. This fact and equation (3.4) imply the validity of the proposition. ■

Note that if γ is simple (i.e. injective), the curve $\mathcal{C} = \bigcup_{k \in \mathbb{Z}} (\gamma([0, 1]) + kz^\perp)$ splits \mathbb{R}^2 into two. We refer to such curves as cuts.

We will use proposition 3.1 in the following form.

Corollary 3.2. *Assume that in addition to the conditions of proposition 3.1, $\dot{\gamma}(s)$ is either parallel or perpendicular to $e(\gamma(s))$ for all s where $\dot{\gamma}(s)$ is defined. Let $T = \{\gamma(s) : \dot{\gamma}(s) \text{ is parallel to } e(\gamma(s))\}$ and $P = \{\gamma(s) : \dot{\gamma}(s) \text{ is perpendicular to } e(\gamma(s))\}$. Then, for any admissible stress field σ ,*

$$\langle \sigma \rangle \cdot z \leq |T| + M|P|, \quad (3.5)$$

where $|T|$ and $|P|$ are the lengths of T and P , respectively.

The validity of this corollary follows from the fact that the integral in equation (3.2) is equal to the right-hand side of (3.5) if γ satisfies the conditions of the corollary.

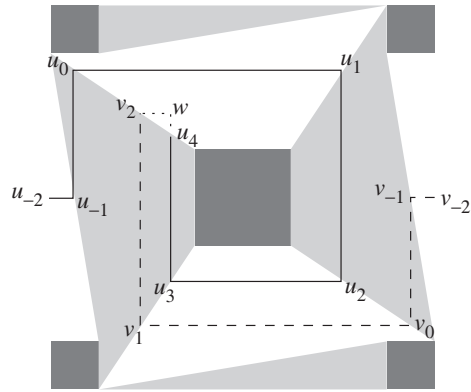


Figure 2. The cut to be used to compute the upper bounds.

(b) The cut

We introduce some notation for convenience. If $x, y \in \mathbb{R}^2$, $[x, y]$ is the closed straight segment that joins x and y and $|x, y|$ denotes its length. We denote by p the function defined on the integers that satisfies $p(i) = i$ if $1 \leq i \leq 4$ and $p(i + 4) = p(i)$ for all i .

Figure 2 shows the period cell $Q = [-1, 1]^2$ of the texture described in § 2 (see also figure 1). It also shows three curves: a solid curve \mathcal{U} , a dashed curve \mathcal{V} and a dotted curve \mathcal{W} . To describe these curves, we introduce the sequence $(s_i)_{0 \leq i}$, where $s_0 = 1 - a$ and $s_{i+1} = g(s_i)$ if $i \geq 0$ (the parameter a was introduced in figure 1 and the function g in equation (2.1)).

The curve \mathcal{U} is given by

$$\mathcal{U} = \bigcup_{i=-1}^{n+1} [u_{i-1}, u_i], \tag{3.6}$$

where $u_{-2} = (-1, 0)$, $u_{-1} = (-1 + a, 0)$ and $u_i = z_{p(i)}(s_i)$ for $0 \leq i \leq n + 1$ (the definition z_k was given in equation (2.1)). Note that for each value of n we have a different curve \mathcal{U} ; for example, in figure 2, $n = 3$.

The curve \mathcal{V} is given by

$$\mathcal{V} = \bigcup_{i=-1}^{n-1} [v_{i-1}, v_i], \tag{3.7}$$

where $v_{-2} = -u_{-2} = (1, 0)$, $v_{-1} = -u_{-1} = (1 - a, 0)$ and $v_i = -u_i = z_{p(i+2)}(s_i)$ for $0 \leq i \leq n - 1$; the curve \mathcal{W} is given by

$$\mathcal{W} = [u_{n+1}, w] \cup [w, v_{n-1}], \tag{3.8}$$

where w is defined by the facts that it belongs to the straight line that contains u_n and u_{n+1} and $[w, v_{n-1}]$ is perpendicular to $[u_{n+1}, w]$.

Note that the union of these curves, which we denote by $\mathcal{L} = \mathcal{U} \cup \mathcal{V} \cup \mathcal{W}$, defines a simple curve whose end points are $(-1, 0)$ and $(1, 0)$. As figure 2 suggests, $P = \{x \in \mathcal{L} : \text{the tangent to } \mathcal{L} \text{ at } x \text{ is perpendicular to } e(x)\} = [u_{n+1}, w]$ and $T = \{x \in \mathcal{L} : \text{the tangent to } \mathcal{L} \text{ at } x \text{ is parallel to } e(x)\} = \mathcal{L} - [u_{n+1}, w] - \text{finite number of points}$.

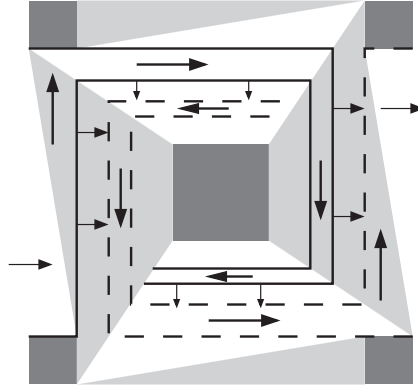


Figure 3. Cartoon of the admissible stress field used in the derivation of the inner bound.

(c) *Outer bounds*

The preceding discussion and corollary 3.2 imply that, for any admissible stress field σ , we have

$$\langle \sigma \rangle \cdot (0, -2) \leq M|w, u_{n+1}| + |v_{n-1}, w| + \sum_{i=-1}^{n+1} |u_{i-1}, u_i| + \sum_{i=-1}^{n-1} |v_{i-1}, v_i|. \quad (3.9)$$

Simple calculations show the following:

$$\left. \begin{aligned} |u_{-2}, u_{-1}| &= a, \\ |u_{-1}, u_0| &= s_1, \\ |u_{i-1}, u_i| &= s_{i-1} + s_{i+1}, \end{aligned} \right\} 0 \leq i, \quad \left. \begin{aligned} |u_{n+1}, w| &= s_n - s_{n+2}, \\ |w, v_{n-1}| &= s_{n-1} - s_{n+1}, \\ |u_{i-1}, u_i| &= |v_{i-1}, v_i|, \end{aligned} \right\} \text{for all } i. \quad (3.10)$$

Thus, equations (3.9) and (3.10), the fact that the texture is invariant under rotation by $\pi/2$, the convexity of K_{hom} , and simple calculations imply

$$K_{\text{hom}} \subseteq \left\{ \tau \in \mathbb{R}^2 : \|\tau\|_\infty \leq M \frac{s_n - s_{n+2}}{2} + 1 + 2 \sum_{i=1}^n s_i \right\} \quad (3.11)$$

(recall that $\|\tau\|_\infty = \max\{|\tau_1|, |\tau_2|\}$). Note that the bound (3.11) depends on the function g , the parameters a and b and the integer n . In § 5 we will compute bounds for different polycrystals (i.e. various choices of g, a, b).

4. Inner bound

Stress fields can be regarded as velocity fields of an incompressible fluid with constant density. In this context the equation (1.2) is due to conservation of mass. To derive our inner bound we will construct an admissible velocity field with the property that a large amount of fluid per unit time will enter the period cell Q from its left-hand side and exit through its the right-hand side. The arrows in figure 3 show the approximate direction and intensity of this velocity field. The two solid curves and the two dashed curves are the union of segments that are parallel to $e(x)$. Fluid enters the tubular region enclosed by the solid curves trough the left-hand side of Q . As we follow this

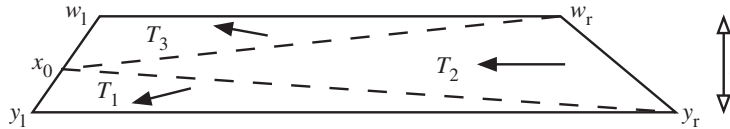


Figure 4. Polygon \mathcal{P} of observation 4.1. The arrows show the direction of σ .

tubular region in the direction of the flow, its width decreases towards zero. Since the velocity is limited by the restrictions (3.1), conservation of mass implies that fluid has to exit this tubular region. However, since the solid curves are parallel to $e(x)$ and given the restrictions (3.1), the rate at which fluid can cross these curves per unit length is one. These facts will limit the rate (per unit time) at which fluid can enter this tubular region through the left-hand side of Q . As fluid leaves the tubular region enclosed by the solid curves, it goes towards the tubular region enclosed by the dashed lines, it enters this region and flows towards the right-hand side of Q . The rest of this section is a detail analysis of this informal discussion.

Spiral flows have also appeared in other contexts. We refer the reader to Bhat-tacharya *et al.* (1999) for an example.

(a) Preliminaries

Our analysis will make use of the following observations.

Observation 4.1 Let \mathcal{P} be a polygon whose boundary is $\partial\mathcal{P} = [y_r, y_l] \cup [y_l, w_l] \cup [w_l, w_r] \cup [w_r, y_r]$ (see figure 4). Assume that the segments $[y_r, y_l]$ and $[w_r, w_l]$ are parallel. Also assume that $0 \leq (w_l - y_l) \cdot (y_r - y_l) \leq (y_r - y_l) \cdot (y_r - y_l)$. Let I be the distance from $[y_r, y_l]$ to $[w_r, w_l]$. Let $t = (y_l - y_r) / \|y_l - y_r\|_2$, where we have used the notation

$$\|(x, y)\|_2 = \sqrt{x^2 + y^2}.$$

For any $\lambda \geq 0$ and any $0 \leq f \leq 1$ there exists a divergence-free field σ defined in \mathcal{P} that satisfies

$$|\sigma(x) \cdot t| \leq \lambda + I^{-1}(f|w_l, w_r| + |y_l, y_r|) \quad \text{and} \quad |\sigma(x) \cdot t^\perp| \leq 1 \tag{4.1}$$

for all $x \in \mathcal{P}$, and

$$\sigma(x) \cdot \hat{n}(x) = \begin{cases} |y_l, w_l|^{-1} \lambda I & \text{if } x \in [y_l, w_l], \\ f & \text{if } x \in [w_l, w_r], \\ 1 & \text{if } x \in [y_l, y_r], \\ -|y_r, w_r|^{-1} (\lambda I + f|w_l, w_r| + |y_l, y_r|) & \text{if } x \in [y_r, w_r], \end{cases} \tag{4.2}$$

where $\hat{n}(x)$ is the vector of norm one perpendicular to $\partial\mathcal{P}$ at x that points in the outward direction, \mathcal{P} .

Proof. Without loss of generality and to simplify the notation, we assume that $y_r - y_l = (|y_r, y_l|, 0)$ and $w_l - y_l = (\alpha, I)$. Note that $0 \leq \alpha \leq |y_l, y_r|$. Let

$$x_0 = \frac{|y_l, y_r| w_l + |w_l, w_r| f y_l}{|w_l, w_r| f + |y_l, y_r|}. \tag{4.3}$$

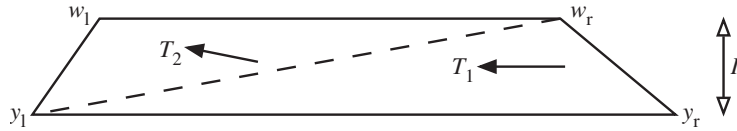


Figure 5. Polygon \mathcal{P} of observation 4.2. The arrows show the direction of σ .

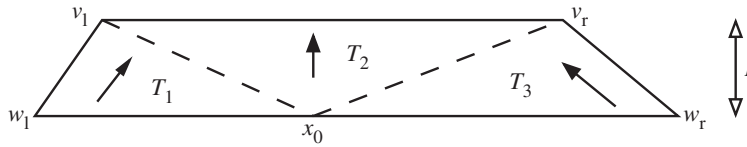


Figure 6. Polygon \mathcal{Q} of observation 4.3. The arrows show the direction of σ .

The dashed lines in figure 4 are two straight segments with x_0 as a common vertex. These lines and $\partial\mathcal{P}$ determine three triangles that we denote by T_i ($1 \leq i \leq 3$). We define

$$\sigma(x) = \begin{cases} -(\lambda + I^{-1}\alpha, 1) & \text{if } x \in T_1, \\ -(\lambda + I^{-1}(f|w_1, w_r| + |y_1, y_r|), 0) & \text{if } x \in T_2, \\ (-\lambda + I^{-1}\alpha f, f) & \text{if } x \in T_3. \end{cases} \quad (4.4)$$

It can be shown that σ is divergence free and satisfies both (4.1) and (4.2). ■

Observation 4.2 Let \mathcal{P} be a polygon whose boundary is $\partial\mathcal{P} = [y_r, y_1] \cup [y_1, w_1] \cup [w_1, w_r] \cup [w_r, y_r]$ (see figure 5). Assume that the segments $[y_r, y_1]$ and $[w_r, w_1]$ are parallel. Also assume that $0 \leq (w_1 - y_1) \cdot (y_r - y_1) \leq (y_r - y_1) \cdot (y_r - y_1)$. Let I be the distance from $[y_r, y_1]$ to $[w_r, w_1]$. Let $t = (y_1 - y_r)/\|y_1 - y_r\|_2$.

For any $0 \leq f \leq 1$ and any $\lambda \geq |y_r, y_1|/(2I)$ there exists a divergence-free field σ defined in \mathcal{P} that satisfies

$$|\sigma(x) \cdot t| \leq \lambda + I^{-1}f|w_1, w_r| \quad \text{and} \quad |\sigma(x) \cdot t^\perp| \leq 1 \quad (4.5)$$

for all $x \in \mathcal{P}$, and

$$\sigma(x) \cdot \hat{n}(x) = \begin{cases} |y_1, w_1|^{-1}\lambda I & \text{if } x \in [y_1, w_1], \\ f & \text{if } x \in [w_1, w_r], \\ 0 & \text{if } x \in [y_1, y_r], \\ -|y_r, w_r|^{-1}(\lambda I + f|w_1, w_r|) & \text{if } x \in [y_r, w_r]. \end{cases} \quad (4.6)$$

Proof. Assuming that $w_r - w_1 = (|w_r, w_1|, 0)$ and $w_1 - y_1 = (\alpha, I)$, we have that $0 \leq \alpha \leq |y_1, y_r|$. Let T_1 and T_2 be the triangles displayed in figure 5. We define

$$\sigma(x) = \begin{cases} -(\lambda + I^{-1}f|w_1, w_r|, 0) & \text{if } x \in T_1, \\ (-\lambda + I^{-1}\alpha f, f) & \text{if } x \in T_2. \end{cases} \quad (4.7)$$

It can be shown that σ is divergence free and satisfies both (4.5) and (4.6). ■

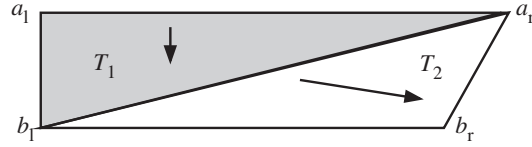


Figure 7. Polygon \mathcal{R} of observation 4.4. The arrows show the direction of σ .

Observation 4.3 Let \mathcal{Q} be a polygon whose boundary is $\partial\mathcal{Q} = [w_r, w_1] \cup [w_1, v_1] \cup [v_1, v_r] \cup [v_r, w_r]$ (see figure 6). Assume that the segments $[w_r, w_1]$ and $[v_r, v_1]$ are parallel. Also assume that $0 \leq (v_1 - w_1) \cdot (w_r - w_1)$ and $0 \leq (v_r - w_r) \cdot (w_1 - w_r)$. Let I be the distance from $[w_r, w_1]$ to $[v_r, v_1]$. Let $t = (w_1 - w_r) / \|w_1 - w_r\|_2$.

There exists a divergence-free field σ defined in \mathcal{Q} that satisfies

$$|\sigma(x) \cdot t| \leq I^{-1}(|w_r, w_1| - |v_r, v_1|) \quad \text{and} \quad |\sigma(x) \cdot t^\perp| \leq 1 \tag{4.8}$$

for all $x \in \mathcal{Q}$, and

$$\sigma(x) \cdot \hat{n}(x) = \begin{cases} 1 & \text{if } x \in [v_r, v_1], \\ 0 & \text{if } x \in [w_1, v_1] \cup [v_r, w_r], \\ -|w_r, w_1|^{-1}|v_r, v_1| & \text{if } x \in [w_r, w_1]. \end{cases} \tag{4.9}$$

Proof. Assume that $w_r - w_1 = (|w_r, w_1|, 0)$ and $v_1 - w_1 = (\alpha_1, I)$. We have that $v_r - w_r = (-\alpha_r, I)$ and $0 \leq \alpha_1, 0 \leq \alpha_r$ satisfy $\alpha_1 + \alpha_r + |v_r, v_1| = |w_r, w_1|$. Let

$$x_0 = \frac{\alpha_r w_1 + \alpha_1 w_r}{\alpha_r + \alpha_1}. \tag{4.10}$$

The dashed lines in figure 6 are two straight segments with x_0 as a common vertex. These lines and $\partial\mathcal{Q}$ determine three triangles denoted by T_i ($1 \leq i \leq 3$). We define

$$\sigma(x) = \begin{cases} |w_r, w_1|^{-1}|v_r, v_1|(I^{-1}\alpha_1, 1) & \text{if } x \in T_1, \\ (0, 1) & \text{if } x \in T_2, \\ |w_r, w_1|^{-1}|v_r, v_1|(-I^{-1}\alpha_r, 1) & \text{if } x \in T_3. \end{cases} \tag{4.11}$$

It can be shown that σ is divergence free and satisfies both (4.8) and (4.9). ■

Observation 4.4 Let \mathcal{R} be a polygon whose boundary is $\partial\mathcal{R} = [a_r, a_1] \cup [a_1, b_1] \cup [b_1, b_r] \cup [b_r, a_r]$ (see figure 7). Assume that the segments $[a_r, a_1]$ and $[b_r, b_1]$ are parallel and the segments $[a_r, a_1]$ and $[a_1, b_1]$ are perpendicular. Also assume that $|a_1, a_r| > |a_1, b_1|$ and $|a_1, a_r| > |b_1, b_r|$. Let T_1 be the triangle whose vertices are $\{a_r, a_1, b_1\}$ and T_2 the triangle whose vertices are $\{b_1, b_r, a_r\}$. Let $t(x)$ be the vector field defined by

$$t(x) = \begin{cases} \|b_1 - a_1\|_2^{-1}(b_1 - a_1) & \text{if } x \in T_1, \\ \|b_r - b_1\|_2^{-1}(b_r - b_1) & \text{if } x \in T_2. \end{cases} \tag{4.12}$$

For any $0 \leq f \leq 1$ and any

$$\alpha \geq \max \left\{ \frac{|a_1, a_r|}{|a_1, b_1|}, \frac{|b_1, b_r|}{|a_1, a_r| - |a_1, b_1|} \right\},$$

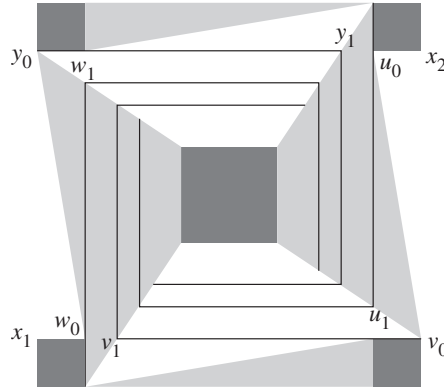


Figure 8. Sequences $(u_i)_{0 \leq i}$, $(v_i)_{0 \leq i}$, $(w_i)_{0 \leq i}$ and $(y_i)_{0 \leq i}$.

there exists a divergence-free field σ defined in \mathcal{R} that satisfies

$$|\sigma(x) \cdot t(x)| \leq \alpha \quad \text{and} \quad |\sigma(x) \cdot t(x)^\perp| \leq 1 \tag{4.13}$$

for all $x \in \mathcal{R}$, and

$$\sigma(x) \cdot \hat{n}(x) = \begin{cases} |a_r, b_r|^{-1} \alpha |a_l, b_l| & \text{if } x \in [a_r, b_r], \\ f & \text{if } x \in [b_l, b_r], \\ 0 & \text{if } x \in [a_l, b_l], \\ -|a_l, a_r|^{-1} (\alpha |a_l, b_l| + f |b_l, b_r|) & \text{if } x \in [a_l, a_r]. \end{cases} \tag{4.14}$$

Proof. Let $v = \|b_l - a_l\|_2^{-1} (b_l - a_l)$. We define

$$\sigma(x) = \begin{cases} |a_l, a_r|^{-1} (\alpha |a_l, b_l| + f |b_l, b_r|) t(x) & \text{if } x \in T_1, \\ f v + (\alpha - |a_l, b_l|^{-1} f (|a_l, a_r| - |b_l, b_r|)) t(x) & \text{if } x \in T_2. \end{cases} \tag{4.15}$$

It can be shown that σ is divergence free and satisfies (4.13) and (4.14). ■

(b) Family of polygons in Q

We will now define a family of polygons included in Q that will be used to obtain our inner bounds.

We denote by q the function defined on the integers that satisfies $q(i) = i + 1$ if $0 \leq i \leq 3$ and $q(i + 4) = q(i)$ for all i . We recall that $(t_i)_{0 \leq i}$ is the sequence defined as $t_0 = 1$ and $t_{i+1} = g(t_i)$ for $i \geq 0$. We will also make use of the functions z_k ($1 \leq k \leq 4$) defined in equation (2.1).

We define the sequences $u_0 = (t_1, t_1)$, $u_i = z_{q(i)}(t_i)$ ($1 \leq i$); $v_i = z_{q(i+1)}(t_i)$ ($0 \leq i$); $w_0 = -(t_1, t_1)$, $w_i = z_{q(i+2)}(t_i)$ ($1 \leq i$); and $y_i = z_{q(i+3)}(t_i)$ ($0 \leq i$) (see figure 8).

For each $i \geq 0$, we denote by \mathcal{P}_i the convex hull of $\{y_i, y_{i+1}, w_{i+1}, w_{i+2}\}$ (i.e. the polygon with vertices $\{y_i, y_{i+1}, w_{i+1}, w_{i+2}\}$), and analogously we define \mathcal{Q}_i as the convex hull of $\{w_i, w_{i+1}, v_{i+1}, v_{i+2}\}$, \mathcal{S}_i as the convex hull of $\{v_i, v_{i+1}, u_{i+1}, u_{i+2}\}$, and \mathcal{T}_i as the convex hull of $\{u_i, u_{i+1}, y_{i+1}, y_{i+2}\}$.

We denote by I_i the distance from $[y_i, y_{i+1}]$ to $[w_{i+1}, w_{i+2}]$. Note that I_i is also equal to the distance from $[w_i, w_{i+1}]$ to $[v_{i+1}, v_{i+2}]$, the distance from $[v_i, v_{i+1}]$ to

$[u_{i+1}, u_{i+2}]$, and the distance from $[u_i, u_{i+1}]$ to $[y_{i+1}, y_{i+2}]$. It can be shown that

$$I_i = t_{i+1} - t_{i+2} \quad \text{for } i \geq 0. \tag{4.16}$$

We will also need the following formulae:

$$\left. \begin{aligned} |y_i, y_{i+1}| = |w_i, w_{i+1}| = |v_i, v_{i+1}| = |u_i, u_{i+1}| = t_i + t_{i+2} \quad \text{if } i \geq 1, \\ |y_0, y_1| = |v_0, v_1| = t_0 + t_2, \quad |w_0, w_1| = |u_0, u_1| = t_1 + t_2. \end{aligned} \right\} \tag{4.17}$$

We note that $e(x) = e(\theta(x))$ is parallel to $[y_i, y_{i+1}]$ and $[w_{i+1}, w_{i+2}]$ for all $x \in \mathcal{P}_i$, $e(x)$ is parallel to $[w_i, w_{i+1}]$ and $[v_{i+1}, v_{i+2}]$ for all $x \in \mathcal{Q}_i$, $e(x)$ is parallel to $[v_i, v_{i+1}]$ and $[u_{i+1}, u_{i+2}]$ for all $x \in \mathcal{S}_i$, and $e(x)$ is parallel to $[u_i, u_{i+1}]$ and $[y_{i+1}, y_{i+2}]$ for all $x \in \mathcal{T}_i$.

We also define \mathcal{R}_1 to be the convex hull of $\{y_0, w_0, w_1, x_1\}$, where $x_1 = (-1, -1 + 2a)$, and \mathcal{R}_2 the convex hull of $\{x_2, u_0, v_0, u_1\}$, where $x_2 = (1, 1 - 2a)$. Note that $\mathcal{R}_2 = -\mathcal{R}_1$ (see figure 8).

(c) *Divergence-free fields in the polygons*

We will now define a divergence-free field within each of the polygons introduced in § 4 b. Some of these divergence-free fields will depend on parameters which will be chosen later in this section.

Let $0 \leq f_0 \leq 1$ and $\lambda_0 \geq |y_0, y_1|/(2I_0)$. We define σ_0^p to be a divergence-free field defined in \mathcal{P}_0 that satisfies

$$|\sigma_0^p(x) \cdot e(x)| \leq \lambda_0 + I_0^{-1} f_0 |w_2, w_1| \quad \text{and} \quad |\sigma_0^p(x) \cdot e(x)^\perp| \leq 1 \tag{4.18}$$

for all $x \in \mathcal{P}_0$ and

$$\sigma_0^p(x) \cdot \hat{n}(x) = \begin{cases} |y_1, w_2|^{-1} \lambda_0 I_0 & \text{if } x \in [y_1, w_2], \\ f_0 & \text{if } x \in [w_2, w_1], \\ 0 & \text{if } x \in [y_1, y_0], \\ -|y_0, w_1|^{-1} (\lambda_0 I_0 + f_0 |w_2, w_1|) & \text{if } x \in [w_1, y_0]. \end{cases} \tag{4.19}$$

The existence of σ_0^p is guaranteed by observation 4.2. More precisely, apply observation 4.2 with $\mathcal{P} = \mathcal{P}_0$, $y_l = y_1$, $y_r = y_0$, $w_l = w_2$, $w_r = w_1$, $f = f_0$ and $\lambda = \lambda_0$.

Let $\lambda_i \geq 0$ and $0 \leq f_i \leq 1$ ($i \geq 1$). We denote by σ_i^p a divergence-free field defined in \mathcal{P}_i that satisfies

$$|\sigma_i^p \cdot e| \leq \lambda_i + I_i^{-1} (f_i |w_{i+2}, w_{i+1}| + |y_{i+1}, y_i|) \quad \text{and} \quad |\sigma_i^p \cdot e^\perp| \leq 1 \tag{4.20}$$

for all $x \in \mathcal{P}_i$ and

$$\sigma_i^p \cdot \hat{n} = \begin{cases} |y_{i+1}, w_{i+2}|^{-1} \lambda_i I_i & \text{if } x \in [y_{i+1}, w_{i+2}], \\ f_i & \text{if } x \in [w_{i+2}, w_{i+1}], \\ 1 & \text{if } x \in [y_{i+1}, y_i], \\ -|y_i, w_{i+1}|^{-1} (\lambda_i I_i + f_i |w_{i+2}, w_{i+1}| + |y_{i+1}, y_i|) & \text{if } x \in [w_{i+1}, y_i]. \end{cases} \tag{4.21}$$

The existence of σ_i^p results from observation 4.1. More precisely, apply observation 4.1 with $\mathcal{P} = \mathcal{P}_i$, $y_l = y_{i+1}$, $y_r = y_i$, $w_l = w_{i+2}$, $w_r = w_{i+1}$, $f = f_i$ and $\lambda = \lambda_i$.

We introduce the divergence-free field σ_i^q ($i \geq 0$), defined in \mathcal{Q}_i , which satisfies

$$|\sigma_i^q(x) \cdot e(x)| \leq I_i^{-1}(|w_i, w_{i+1}| - |v_{i+1}, v_{i+2}|) \quad \text{and} \quad |\sigma_i^q(x) \cdot e(x)^\perp| \leq 1 \quad (4.22)$$

for all $x \in \mathcal{Q}_i$ and

$$\sigma_i^q(x) \cdot \hat{n}(x) = \begin{cases} 1 & \text{if } x \in [v_{i+1}, v_{i+2}], \\ 0 & \text{if } x \in [w_{i+1}, v_{i+2}] \cup [v_{i+1}, w_i], \\ -|w_i, w_{i+1}|^{-1}|v_{i+1}, v_{i+2}| & \text{if } x \in [w_i, w_{i+1}]. \end{cases} \quad (4.23)$$

The existence of σ_i^q is a consequence of observation 4.3. More precisely, apply observation 4.3 with $\mathcal{Q} = \mathcal{Q}_i$, $w_l = w_{i+1}$, $w_r = w_i$, $v_l = v_{i+2}$ and $v_r = v_{i+1}$.

We define σ_i^s ($i \geq 0$) in \mathcal{S}_i as $\sigma_i^s(x) = \sigma_i^p(-x)$. Note that σ_i^s is well defined because $\mathcal{S}_i = -\mathcal{P}_i$ and σ_i^s is divergence free within \mathcal{S}_i . Analogously we have $\sigma_i^t(x) = \sigma_i^q(-x)$ for all $x \in \mathcal{T}_i$ ($i \geq 0$).

Finally, let $0 \leq h \leq 1$ and $\beta \geq \max\{|x_1, y_0|/|x_1, w_0|, |w_0, w_1|/(|x_1, y_0| - |x_1, w_0|)\}$; we denote by σ_1^r a divergence-free field defined in \mathcal{R}_1 that satisfies

$$|\sigma_1^r(x) \cdot e(x)| \leq \beta \quad \text{and} \quad |\sigma_1^r(x) \cdot e(x)^\perp| \leq 1 \quad (4.24)$$

for all $x \in \mathcal{R}_1$, and

$$\sigma_1^r(x) \cdot \hat{n}(x) = \begin{cases} |y_0, w_1|^{-1}\beta|w_0, x_1| & \text{if } x \in [y_0, w_1], \\ h & \text{if } x \in [w_0, w_1], \\ 0 & \text{if } x \in [w_0, x_1], \\ -|x_1, y_0|^{-1}(\beta|w_0, x_1| + h|w_0, w_1|) & \text{if } x \in [x_1, y_0], \end{cases} \quad (4.25)$$

and we denote by σ_2^r the divergence-free field defined in \mathcal{R}_2 given by $\sigma_2^r(x) = \sigma_1^r(-x)$. Note that the existence of σ_1^r results from observation 4.4. More precisely, apply observation 4.4 with $\mathcal{R} = \mathcal{R}_1$, $a_l = x_1$, $a_r = y_0$, $b_l = w_0$, $b_r = w_1$ and $\beta = \alpha$.

(d) *A family of stress fields*

We will now define a family of stress fields that will be used to obtain our inner bounds. More precisely, for each integer $k \geq 2$ we define in $Q = [-1, 1]^2$ a field σ as

$$\sigma(x) = \begin{cases} \sigma_i^p(x) & \text{if } x \in \mathcal{P}_i \text{ and } 0 \leq i \leq k, \\ \sigma_i^q(x) & \text{if } x \in \mathcal{Q}_i \text{ and } 0 \leq i \leq k-1, \\ \sigma_i^s(x) & \text{if } x \in \mathcal{S}_i \text{ and } 0 \leq i \leq k, \\ \sigma_i^t(x) & \text{if } x \in \mathcal{T}_i \text{ and } 0 \leq i \leq k-1, \\ \sigma_1^r(x) & \text{if } x \in \mathcal{R}_1, \\ \sigma_2^r(x) & \text{if } x \in \mathcal{R}_2, \\ 0 & \text{otherwise,} \end{cases} \quad (4.26)$$

and we extend the definition of σ to \mathbb{R}^2 so that it becomes Q -periodic.

Elementary calculations show that there is a unique set of parameters λ_i, f_i, h and β that makes σ divergence free. More precisely, the continuity of the normal component of σ at $[w_i, w_{i+1}]$ ($0 \leq i \leq k+1$) implies

$$\left. \begin{aligned} h &= |w_0, w_1|^{-1} |v_1, v_2|, \\ f_i &= |w_{i+2}, w_{i+1}|^{-1} |v_{i+3}, v_{i+2}| \quad \text{if } 0 \leq i \leq k-2, \\ f_{k-1} &= f_k = 0, \end{aligned} \right\} \quad (4.27)$$

and the continuity of the normal component of σ at $[y_i, w_{i+1}]$ ($k+1 \geq i \geq 0$) implies

$$\left. \begin{aligned} \lambda_k &= 0, \\ \lambda_i I_i &= \lambda_{i+1} I_{i+1} + f_{i+1} |w_{i+3}, w_{i+2}| + |y_{i+2}, y_{i+1}| \quad \text{if } k-1 \geq i \geq 0, \\ 2a\beta &= \lambda_0 I_0 + f_0 |w_2, w_1|. \end{aligned} \right\} \quad (4.28)$$

Given the above choice of the parameters, it can be shown that σ is divergence free everywhere in \mathbb{R}^2 . Note that each f_i satisfies the constraint $0 \leq f_i \leq 1$. It is also easy to verify that $\lambda_i \geq 0$ for all i . In the definition of σ_0^p and σ_1^r we imposed restrictions on both β and λ_0 . In all the examples to be considered in this paper those restrictions will be satisfied.

(e) *Admissibility of the stress fields*

For each value of M , we will select an integer $k = k(M)$ so that the stress field σ defined in equation (4.26) will result admissible and will produce the desired inner bound. To that end we first obtain the parameters λ_i, f_i, h and β in terms of the parameters t_i . Equations (4.17) and (4.27) imply that

$$\left. \begin{aligned} h &= (t_1 + t_2)^{-1} (t_1 + t_3), \\ f_i &= (t_{i+1} + t_{i+3})^{-1} (t_{i+2} + t_{i+4}) \quad \text{if } 0 \leq i \leq k-2, \\ f_{k-1} &= f_k = 0. \end{aligned} \right\} \quad (4.29)$$

Equations (4.16), (4.17), (4.28) and (4.29) and elementary calculations imply

$$\left. \begin{aligned} \lambda_i (t_{i+1} - t_{i+2}) &= \sum_{j=i+1}^k (t_j + t_{j+2}) + \sum_{j=i+3}^k (t_j + t_{j+2}) \quad \text{if } k-1 \geq i \geq 0, \\ 2a\beta &= \sum_{j=1}^k (t_j + t_{j+2}) + \sum_{j=2}^k (t_j + t_{j+2}) \end{aligned} \right\} \quad (4.30)$$

(we use the standard convention that $\sum_{j=m}^n a_j = 0$ if $n < m$).

We now obtain a restriction on k that will guarantee admissibility of σ . σ satisfies (3.1) within \mathcal{P}_i and \mathcal{S}_i , for $1 \leq i \leq k$, if the right-hand side of the first equation in (4.20) is bounded by M . This condition in terms of the parameters t_i reduces to

$$\sum_{j=i}^k t_j + t_{j+2} + \sum_{j=i+2}^k t_j + t_{j+2} \leq M(t_{i+1} - t_{i+2}). \quad (4.31)$$

Similarly, σ satisfies (3.1) within \mathcal{P}_0 and \mathcal{S}_0 if

$$\sum_{j=1}^k t_j + t_{j+2} + \sum_{j=2}^k t_j + t_{j+2} \leq M(t_1 - t_2) \quad (4.32)$$

(see equation (4.18)) and σ satisfies (3.1) within \mathcal{R}_1 and \mathcal{R}_2 if

$$\sum_{j=1}^k t_j + t_{j+2} + \sum_{j=2}^k t_j + t_{j+2} \leq M2a. \quad (4.33)$$

Thus, if k is chosen so that (4.31)–(4.33) are satisfied, σ is admissible. The larger the k , the larger the average of the stress field σ . Since we want our inner bound to be as large as possible, once we consider our examples and specify g , we will maximize k subject to the restrictions (4.31)–(4.33).

(f) *Average of the stress fields*

The average of the stress σ introduced in §4d can be obtained by applying equation (3.4) with cut $x = -1$ and cut $y = -1$. Simple calculations show that

$$\langle \sigma \rangle = (a\beta + \frac{1}{2}(t_1 + t_3))(1, 0). \quad (4.34)$$

(g) *Inner bound*

Equations (4.30) and (4.34), and the facts that the texture has square symmetry and that K_{hom} is convex imply

$$\left\{ \tau \in \mathbb{R}^2 : \|\tau\|_1 \leq \sum_{j=1}^k (t_j + t_{j+2}) \right\} \subseteq K_{\text{hom}}, \quad (4.35)$$

as long as equations (4.31)–(4.33) are satisfied.

5. Examples

In this section we will use the results of §§3 and 4 to obtain inner and outer bounds of various polycrystals.

(a) *Straight grain boundaries*

We now consider the case in which the function g (see §2) is linear and thus is given by $g(t) = b + \rho(t - b)$, where $\rho = (1 - 2a - b)/(1 - b)$.

(i) *Outer bound*

We first evaluate the outer bound. Given the function g under consideration, the sequence $(s_i)_{i \geq 0}$ defined in §3b is given by

$$s_i = b + (s_0 - b)\rho^i. \quad (5.1)$$

Thus, we have

$$M \frac{s_n - s_{n+2}}{2} + 2 \sum_{i=1}^n s_i = \frac{1}{2}(s_0 - b)(1 - \rho)^2 \rho^n M + 2nb + 2(s_0 - b)\rho \frac{1 - \rho^n}{1 - \rho}. \tag{5.2}$$

Let n be the smallest integer that satisfies $n \geq -\log M / \log \rho$. Simple calculations show that the right-hand side of equation (5.2) is bounded by $-1 + E_0 - 2b \log M / \log \rho$, where E_0 is a constant that depends on a and b , but it is independent of n and M . Thus, from equation (3.11) we obtain

$$K_{\text{hom}} \subseteq \left\{ \tau \in \mathbb{R}^2 : \|\tau\|_\infty \leq -\frac{2b}{\log \rho} \log M + E_0 \right\}. \tag{5.3}$$

(ii) *Inner bound*

We now turn to the inner bound. The sequence $(t_i)_{i \geq 0}$ defined in § 2 is given by

$$t_i = b + (1 - b)\rho^i. \tag{5.4}$$

Elementary calculations show that the restrictions (4.31) and (4.32) are satisfied if

$$4b(k - i) + 2b + \frac{(1 - b)}{(1 - \rho)} (1 + \rho^2)^2 \leq M(1 - b)(1 - \rho)\rho^{i+1} \tag{5.5}$$

for all $0 \leq i \leq k$. To select the k that will lead to the inner bound, we need the following observation.

Observation 5.1 *Let a_1, a_2, L, λ and u be positive constants. Assume $u < 1$. If*

$$L \leq (\log u)^{-1}(\log a_1 - \log \lambda - \log(-\log u) - 1) - \frac{a_2}{a_1}, \tag{5.6}$$

then

$$a_1(L - x) + a_2 \leq \lambda u^x \quad \text{for all } x. \tag{5.7}$$

Proof. Let $f(x) = \lambda u^x - a_1(L - x) - a_2$. Let x_* be the minimizer of f . Then $f'(x_*) = \lambda u^{x_*} \log u + a_1 = 0$. A simple calculation shows that $f(x_*) \geq 0$ if (5.6) is valid. The validity of the observation follows. ■

From this observation and simple algebra, it follows that we can choose $k \geq -\log M / \log \rho - C$, where C is a constant independent of M and satisfy (5.5) for all M . We note that with this choice of k and in our regime of interest, $M \gg 1$, equation (4.33) is also satisfied. Thus, equations (4.35) and (5.4) imply

$$\left\{ \tau \in \mathbb{R}^2 : \|\tau\|_1 \leq -\frac{2b}{\log \rho} \log M - D_0 \right\} \subseteq K_{\text{hom}}, \tag{5.8}$$

where D_0 is a positive constant independent of M .

(b) *Curved grain boundaries*

Let $0 < r$. We now study the case in which

$$t_i = b + \frac{\eta}{i^r} \quad \text{with } \eta = (1 - 2a - b), \quad (5.9)$$

for $i \geq 1$, where $(t_i)_{i \geq 0}$ is the sequence defined in §2. Recall that the function g is determined by the facts that $g(t_i) = t_{i+1}$ and g is linear within (t_{i+1}, t_i) . It can be shown that g satisfies the restrictions discussed in §2, i.e. $0 < g'(t) < 1$ for all t where g' is defined.

(i) *Outer bound*

First we observe that $s_i = (t_{i+1} + t_i)/2$ for $i \geq 0$ (the sequence $(s_i)_{i \geq 0}$ was defined in §3b). It can thus be shown that

$$M \frac{s_n - s_{n+2}}{2} + 1 + 2 \sum_{i=1}^n s_i = \frac{\eta r}{n^{r+1}} M + 2nb + O\left(h_n + \frac{M}{n^{r+2}}\right), \quad (5.10)$$

where

$$h_n = \begin{cases} 1 & \text{if } r > 1, \\ \log(n) & \text{if } r = 1, \\ n^{1-r} & \text{if } r < 1. \end{cases} \quad (5.11)$$

Minimizing the right-hand side of equation (5.10) with respect to n leads us to choose a value of n that satisfies $2b(n + \delta)^{r+2} = r(r+1)\eta M$ for some δ that satisfies $|\delta| \leq 1/2$. Thus, equations (5.10) and (3.11) imply

$$K_{\text{hom}} \subseteq \left\{ \tau \in \mathbb{R}^2 : \|\tau\|_\infty \leq 2b \frac{(2+r)}{(1+r)} \left(\frac{(1+r)r\eta}{2b} M \right)^{1/(2+r)} + E_r A_M \right\}, \quad (5.12)$$

where

$$A_M = \begin{cases} 1 & \text{if } r > 1, \\ \log(M) & \text{if } r = 1, \\ M^{(1-r)/(2+r)} & \text{if } r < 1, \end{cases} \quad (5.13)$$

and E_r is a constant independent of M .

(ii) *Inner bound*

We now turn to the evaluation of the inner bound. It can be shown that the restrictions (4.31) and (4.32) are satisfied for $i \geq 1$ if

$$2b + k^{-r} 2\eta \leq (k+2)^{-(r+1)} \eta r M, \quad (5.14)$$

$$4b + (k-1)^{-r} 4\eta \leq (k+1)^{-(r+1)} \eta r M, \quad (5.15)$$

$$4(k-i)b + 4\eta h_k \leq (i+2)^{-(r+1)} \eta r M, \quad (5.16)$$

where

$$h_k = \begin{cases} (1-r)^{-1}k^{1-r} & \text{if } r < 1, \\ 1 + \log k & \text{if } r = 1, \\ r/(r-1) & \text{if } r > 1. \end{cases} \quad (5.17)$$

To choose the value of k that will give us our inner bound we need the following observation, whose proof is simple.

Observation 5.2 *Let c, d and λ be positive constants. Assume that $c2^{\lambda+1} \leq d\lambda$. Then*

$$\max \left\{ \eta : \eta - cx \leq \frac{d}{(x+2)^\lambda} \text{ for all } x \geq 0 \right\} = c \frac{\lambda+1}{\lambda} \left(\frac{\lambda d}{c} \right)^{1/(\lambda+1)} - 2c. \quad (5.18)$$

With the help of observation 5.2, it can be shown that the equations (5.14)–(5.16) are satisfied if we set

$$k = \frac{r+2}{r+1} \left(\frac{r(1+r)\eta M}{4b} \right)^{1/(2+r)} - CA_M, \quad (5.19)$$

where C is bounded by a constant independent of M and A_M is given by (5.13). Moreover, the restriction (4.33) is also satisfied in our regime of interest (i.e. $M \gg 1$). This choice of k equations (4.35) and (5.9), the square symmetry of the texture and the convexity of K_{hom} leads to the inner bound

$$\left\{ \tau \in \mathbb{R}^2 : \|\tau\|_1 \leq 2b \frac{(2+r)}{(1+r)} \left(\frac{(1+r)r\eta}{4b} M \right)^{1/(2+r)} - D_r A_M \right\} \subseteq K_{\text{hom}}, \quad (5.20)$$

where D_r is a constant independent of M .

References

- Bhattacharya, K., Kohn, R. V. & Kozlov, S. 1999 Some examples of nonlinear homogenization involving nearly degenerate energies. *Proc. R. Soc. Lond. A* **455**, 567–583.
- Bishop, J. & Hill, R. 1951 A theory for the plastic distortion of a polycrystalline aggregate under combined stresses. *Phil. Mag.* **42**, 414–427.
- Bolton, W. 1996 *Materials and their uses*. Oxford: Butterworth-Heinemann.
- Bouchitté, G. & Suquet, P. 1991 Homogenization, plasticity and yield design. In *Composite media and homogenization* (ed. G. D. Maso & G. Dell’Antonio), pp. 107–133. Birkhäuser.
- de Buhan, P. 1986 Approche fondamentale du calcul à la rupture des ouvrages en sols renforcés. Thèse d’Etat, Université de Paris-VI, France.
- de Buhan, P. & Taliercio, A. 1991 A homogenization approach to the yield strength of composite materials. *Eur. J. Mech. A* **10**, 129–154.
- deBotton, G. & Ponte Castañeda, P. 1995 Variational estimates for the creep behavior of polycrystals. *Proc. R. Soc. Lond. A* **488**, 121–142.
- Demengel, F. & Qi, T. 1990 Convex functions of a measure obtained by homogenization. *SIAM J. Math. Analysis* **21**, 409–435.
- Dendievel, R., Bonnet, G. & Willis, J. R. 1991 Bounds for the creep behavior of polycrystalline materials. In *Inelastic deformations of composite materials* (ed. G. J. Dvorak), pp. 175–192. Springer.

- Goldsztein, G. H. 2001 Rigid perfectly plastic two-dimensional polycrystals. *Proc. R. Soc. Lond. A* **457**, 2789–2798.
- Hirth, J. P. & Lothe, J. 1982 *Theory of dislocations*. New York: McGraw-Hill.
- Hutchinson, J. W. 1976 Bounds and self-consistent estimates for creep of polycrystalline materials. *Proc. R. Soc. Lond. A* **348**, 101–127.
- Jikov, V., Kozlov, S. & Oleinik, O. 1994 *Homogenization of differential operations and integral functionals*. Springer.
- Kohn, R. V. & Little, T. D. 1998 Some model problems of polycrystal plasticity with deficient basic crystals. *SIAM J. Appl. Math.* **59**, 172–197.
- Lebensohn, R. 1993 A self-consistent anisotropic approach for the simulation of plastic-deformation and texture development of polycrystals: application to zirconium alloys. *Acta Metall. Mater.* **41**, 2611–2624.
- Lebensohn, R. 1999 Modeling the role of local correlations in polycrystal plasticity using viscoplastic self-consistent schemes. *Model. Simul. Mater. Sci. Engng* **7**, 739–746.
- Lubliner, J. 1990 *Plasticity theory*. New York: Macmillan.
- Nesi, V., Smyshlyaev, V. P. & Willis, J. R. 2000 Improved bounds for the yield stress of a model polycrystalline material. *J. Mech. Phys. Solids* **48**, 1799–1825.
- Olson, T. 1994 Improvements on Taylor's upper bound for rigid-plastic composites. *Mater. Sci. Engng A* **175**, 15–20.
- Ponte Castañeda, P. 1991 The effective mechanical properties of nonlinear isotropic composites. *J. Mech. Phys. Solids* **39**, 45–71.
- Ponte Castañeda, P. 1996 Exact second-order estimates for the effective mechanical properties of nonlinear composite materials. *J. Mech. Phys. Solids* **44**, 827–862.
- Ponte Castañeda, P. & Nebozhyn, M. 1997 Variational estimates of the self consistent type for some model nonlinear polycrystals. *Proc. R. Soc. Lond. A* **453**, 2715–2724.
- Ponte Castañeda, P. & Suquet, P. 1997 Nonlinear composites. *Adv. Appl. Mech.* **34**, 171–302.
- Sab, K. 1994 Homogenization of non-linear random media by a duality method. Application to plasticity. *Asymp. Analysis* **9**, 311–336.
- Sachs, G. 1928 Zur Ableitung einer Fließbedingung. *Z. Ver. Deutsche Ing.* **72**, 734–736.
- Suquet, P. 1982 Plasticité et homogénéisation. Thèse d'Etat, Université Pierre et Marie Curie, Paris, France.
- Suquet, P. 1983 Analyse limite et homogénéisation. *C. R. Acad. Sci. Paris Sér. II* **296**, 1355–1358.
- Suquet, P. 1987 Elements of homogenization for inelastic solid mechanics. In *Homogenization techniques for composite media* (ed. E. Sanchez-Palencia & A. Zaoui). Lecture Notes in Physics, vol. 272, pp. 193–278. Springer.
- Suquet, P. 1988 Discontinuities and plasticity. In *Nonsmooth mechanics and applications* (ed. J. J. Moreau & P. D. Panagiotopoulos), pp. 278–340. Springer.
- Suquet, P. 1993 Overall potentials and extremal surfaces of power law or ideally plastic materials. *J. Mech. Phys. Solids* **41**, 981–1002.
- Talbot, D. R. S. & Willis, J. R. 1985 Variational principles for inhomogeneous nonlinear media. *IMA J. Appl. Math.* **35**, 39–54.
- Taylor, G. 1938 Plastic strains in metals. *J. Inst. Metals* **62**, 307–324.
- Willis, J. R. 1983 The overall elastic response of composite materials. *J. Appl. Mech.* **50**, 1202–1209.